

# PROBABILITY STUDY FOR A HIGH-CAPACITY MICROPILE BEARING MECHANISM

Yoshinori OTANI<sup>1</sup>, Kei ASAKURA<sup>2</sup>, and Masaru HOSHIYA<sup>2</sup>

<sup>1</sup>Hirose & Co., Ltd.

<sup>2</sup>Musashi Institute of Technology

High-capacity micro-piles are cast in place and heavily depend on construction technique and soil properties. As such, uncertainties regarding the bearing capacity of the piles are involved. Therefore, utmost care must be taken in designing piles to ensure safety. This paper determines the performance function of a pile's push-in bearing capacity under three separate critical conditions: ground subsidence due to the insufficient bearing capacity of a pile, steel-pipe fractures due to compression, and fractures in non-steel-pipe areas due to compression. We examine these uncertainties in terms of probability and study how to use partial factor design in programming the push-in bearing capacity of high capacity micro piles.

**Key words:** High-capacity micro-pile, partial factor design, uncertainty, reliability theory

## 1. Introduction

Piles of 300mm or less that are used on construction sites are generally called 'micro piles' (abbreviated to MPs in this paper). The origin dates back to 1952 when F. Lizzi in Italy developed what was then called the 'root pile'.<sup>1)</sup> Lizzi invented MPs of 150mm or less which are composed of irregularly-shaped steel bars and grout, and are used mainly for adding strength to the supporting capacity of the ground and for underpinning the structures above. Since then MPs have gained popularity all over the world, including the UK,

Germany, France, the USA, and some Asian countries.<sup>2), 3)</sup> MPs were introduced into Japan in 1979, and in 1980 the first MP was placed in Asukayama Tenbodai<sup>4)</sup> in Tokyo. To date, 700 projects have been completed with the use of MPs. In 1971, 1989, and 1994, the State of California in the USA suffered widespread destruction of road bridges due to major earthquakes, and MPs were employed to support bridge foundations and to prevent bridges from collapsing.<sup>5)</sup> Meanwhile, High-Capacity Micro-Piles (abbreviated to HMPs in this paper), which are the focus of the present paper, came into use particularly after the year

Table 1 Shape Standards <sup>10)</sup>

	Type	Standards	Dimensions	Strength/Quality
Supporting Steel Pipe	Oil-Well Pipe	API 5CT, N-80 fsy:80-110ksi (560-760 N/mm <sup>2</sup> )	Outside diameter 178mm thickness 12.7mm	fc=703N/mm <sup>2</sup>
Supporting Reinforcing Bar	twisted reinforcing bar irregularly-shaped steel	SD490 D51	Nominal Diameter 51mm Section Area 20.3 cm <sup>2</sup>	fb=490N/mm <sup>2</sup>
Grout	Cement Paste	W/C=45% Fc = 35N/mm <sup>2</sup>		$f_{28} = 44-58 \text{ N/mm}^2$ (Average $f_{28}=53 \text{ N/mm}^2$ )

1989, when the Loma Prieta earthquake occurred, to add strength to bridge foundations.<sup>6)</sup> In Japan too, HMPs were recognized as a new technology that can be used to improve the anti-earthquake performance of new and existing structures after the Nambu earthquake in Hyogo Prefecture in 1995.<sup>7),8)</sup> One typical project is the Sashiumi Bridge where HMPs were used to strengthen the anti-earthquake capacity of the footings of the bridge.

An HMP is shown in fig. 1; it combines irregularly-shaped reinforcing bars and steel pipes as shown in Tab.1, which makes it possible to have high durability and a high bearing capacity, even for this type of small-diameter pile. The HMP has outstanding advantages: the footing area can be minimized due to the small diameter of the pile when used as a technique to add strength to the anti-earthquake performance of bridge foundations, and the pile is suitable for reinforcing existing structures where construction space is limited. HMPs can be placed using small machines, even when there is a limited clearance of as little as 3.5 meters available above the pile top.<sup>9)</sup>

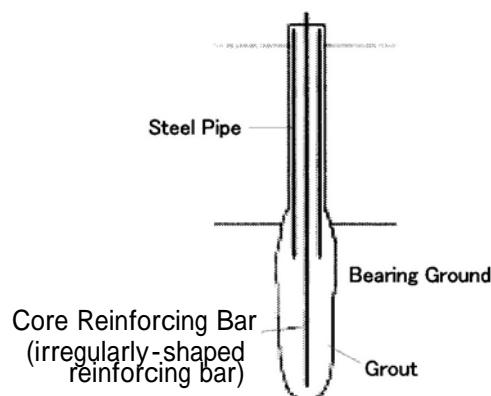


Figure 1 High-Capacity Micro Pile

On the other hand, the HMP is used on construction sites, and its bearing capacity depends greatly on the level of quality control at the construction site. The HMP is also influenced by various elements inherent in the individual ground conditions. As a result, uncertain factors are involved, and in order to ensure safety at the design stage, sufficient consideration must be given to examining the vertical and horizontal bearing capacity, the ground subsidence level etc. and to controlling these uncertain factors.

However, the current design guidelines (proposed) in the Design and Construction Manual (proposed) on HMPs<sup>9)</sup> employs an allowable-stress method, and safety of the allowable push-in bearing capacity, which is a typical

bearing capacity, is computed by using safety factors that are consolidated for the load/strength.

The bearing capacity of the HMP is determined by factors such as the strength of the pile body itself, and the frictional resistance between the surrounding surface of the pile and the ground.

Each of these factors is associated with corresponding uncertain elements. In

order to evaluate these individual uncertain elements quantitatively, safety factors need to be varied depending on fluctuations in the component factors of the HMP bearing capacity.

This paper examines applications of the Partial Factor Design Method <sup>10), 11), 12)</sup> to the design and engineering of the push-in bearing capacity of the HMP based on probability theory.

Partial factor design is a method in

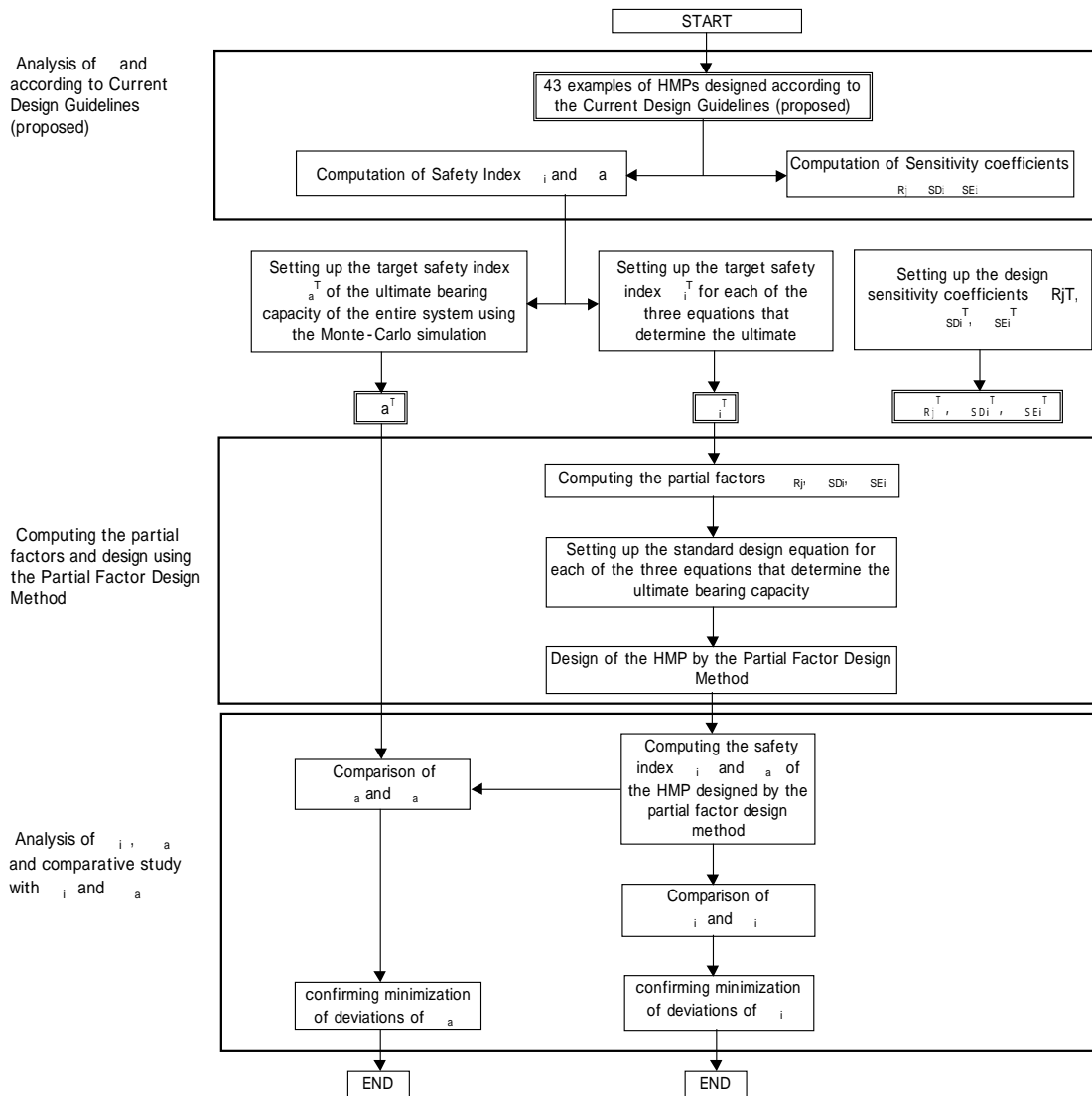


Figure-2 Reliability Analysis of the Push-in Bearing Capacity of the HMP

which different safety coefficients are given to multiple design loads and strengths, and it is employed in Europe and the USA, where globalization of the technology standards for performance/quality design has started. The aims of this paper are: (1) as shown in Figure 2, to carry out a reliability analysis on an actual HMP that was designed based on the Current Design Guidelines (proposed), and to examine the fluctuations in the reliability level of the HMP for this case; (2) to introduce design standards for Partial Factor Design and determine partial factors in compliance with the reliability levels shown in (1); and (3) to make a comparative study of the safety index between examples computed using the Current Design Guidelines, and examples computed using Partial Factor Design, and to demonstrate that Partial Factor Design can produce superior results.

## 2. Current Design Guidelines (proposed) and their problems

(1) Push-in bearing capacity in the Current Design Guidelines (proposed) and critical conditions

The allowable push-in bearing capacity of an HMP,  $R_{ca}$  is given by equation (1) below, according to the Current Design Guidelines (proposed) in the Design and Construction Manual on High-Capacity

Micro Piles (proposed). The ultimate push-in bearing capacity,  $R_{cu}$  given in equation (2), is computed from the minimum values of the three bearing capacities for the corresponding critical conditions.

$$R_{ca} = \frac{rR_{cu}}{n} \quad (1)$$

$r$ : correction coefficient for the safety factor due to the different assumptions in the method used for the ultimate bearing capacity

$n$ : safety factor

$$R_{cu} = \min[R_{c1}, R_{c2}, R_{c3}] \quad (2)$$

$R_{c1}$ : ultimate frictional bearing capacity

$R_{c2}$ : compression strength of the steel pipe section of the pile

$R_{c3}$ : sum of the ultimate compression strength of the non-steel section of the pile and the ultimate frictional resistance of the steel pipe section of the pile

The three critical conditions: condition 1 ( $Z_1 \leq 0$ ); condition 2 ( $Z_2 \leq 0$ ); and condition 3 ( $Z_3 \leq 0$ ) corresponding to  $R_{c1}$ ,  $R_{c2}$  and  $R_{c3}$  are described conceptually in Figure 3, Figure 4, and Figure 5.  $Z_i$  ( $i=1,2, \text{ and } 3$ ) is the performance function of equation (14), equation (15) and equation (16), and  $Z \leq 0$  defines the occurrence of the critical condition  $i$ .

Figure 6 shows the resisting forces  $R_1$  to  $R_7$  of the HMP against the push-in bearing capacity.

Critical condition 1 is a state where

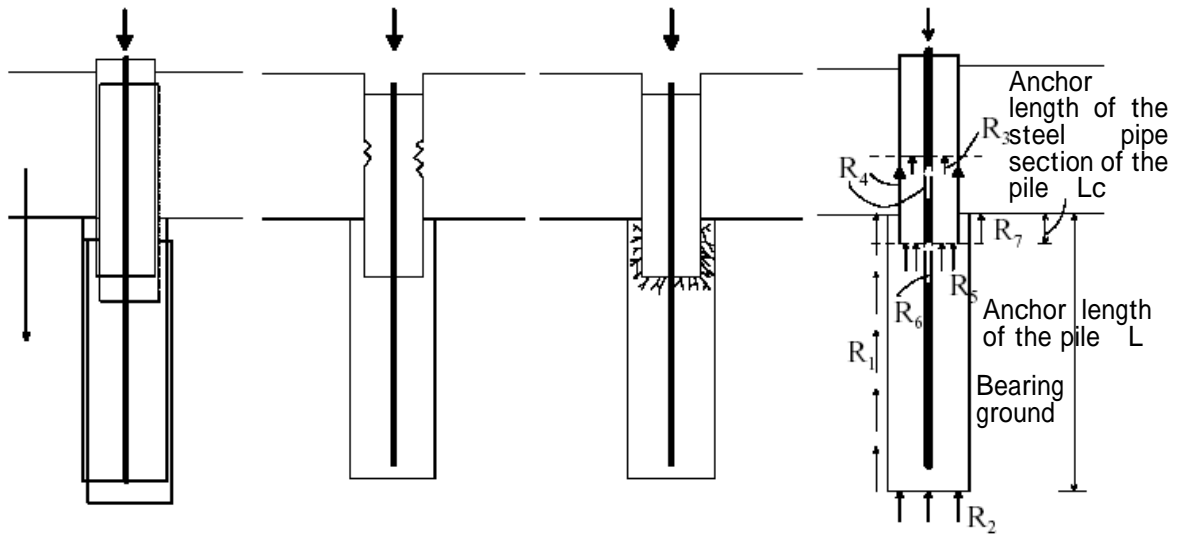


Figure 3  
Conceptual Diagram  
of Limit State 1

Figure 4  
Conceptual Diagram  
of Limit State 2

Figure 5  
Conceptual Diagram  
of Limit State 3

Figure 6  
Outline Diagram  
of Each Resisting  
Force of the HMP

settlement is caused by insufficient bearing capacity of the ground. The force the HMP exerts in resisting this is a combination of the frictional force of the area surrounding the fixed pile,  $R_1$  and the bearing capacity of the deepest bottom of the pile,  $R_2$ . Therefore,  $R_{c1}$  is expressed as the sum of  $R_1$  and  $R_2$ , i.e., as the bearing capacity for critical condition 1, given in equation (5).

$$R_1 = \pi a D_0 \sum \tau_i L_i \quad (3)$$

$$R_2 = q \pi \frac{D_0^2}{4} \quad (4)$$

$$R_{c1} = R_1 + R_2 \quad (5)$$

a: correction coefficient for the pressurization effect of the grout

$D_0$ : diameter of drill hole

$\tau_i$ : Frictional Strength of the perimeter surface of layer (i) of the anchor section that is affected by the frictional forces at the perimeter surface

$L_i$ : Thickness of layer (i) that is affected by the frictional forces at the perimeter surface

q: Ultimate bearing stress per unit area determinable by the subject ground

According to the Current Design Guidelines (proposed) on HMPs, the ultimate frictional bearing capacity  $R_{c1}$  is computed using an equation similar to the one for the ultimate push-in bearing capacity of frictional piles shown in the Design and Construction Guidelines for Roads and Bridges.<sup>13)</sup>

According to the Current Design Guidelines (proposed) for HMPs, the bearing capacity of the bottom section of the small diameter type HMP can be discounted because it is considered that the frictional forces at the perimeter surface  $R_1$  alone constitute a sufficient part of the ultimate strength of the bearing capacity for a more conservative

safety factor. However, this paper takes into account the bottom bearing capacity  $R_2$  and adds it to the ultimate frictional bearing capacity  $R_{c1}$ , in order also to further examine the behavior of  $R_2$ .

Critical Condition 2 shows a compression failure in the steel pipe section of the pile, where the forces of resistance that the HMP generates against this failure consist of the ultimate compression strength of the grout in the steel pipe section of the pile,  $R_3$  and the ultimate compression strength of the reinforcing bars and steel pipe,  $R_4$ .  $R_{c2}$  is expressed by equation (8).

$$R_3 = 0.85f_G A_{G1} \quad (6)$$

$$R_4 = F_{BorC}(A_B + A_C) \quad (7)$$

$$R_{C2} = R_3 + R_4 \quad (8)$$

$f_G$ : Compression strength of grout 28 days after placement

$A_{G1}$ : Effective design sectional area of the grout for the steel pipe section of the pile

$F_{B or C}$ : The lesser of either  $F/B$  or  $F/C$

$F/B$  is the yield strength of the core reinforcing bar

$F/C$  is the yield strength of the steel pipe

$A_B$ : Sectional area of the core reinforcing bar

$A_C$ : Sectional area of the steel pipe

The constant value 0.85 in equations (6) and (9) is the maximum ratio of concrete stress to compression strength  $f_G$  for

standard samples.

Critical Condition 3 shows a compression failure in the non-steel section of the pile. The HMP generates resisting forces  $R_5$ ,  $R_6$  and  $R_7$ .  $R_5$  is the ultimate compression strength of the grout in the non-steel section of the pile.  $R_6$  is the ultimate compression strength of the reinforcing bar, and  $R_7$  is the frictional force at the perimeter surface of the anchor part of the steel section of the pipe. Thus  $R_{c3}$  is

$$R_5 = 0.85f_G A_{G2} \quad (9)$$

$$R_6 = f_B A_B \quad (10)$$

$$R_7 = \pi a D_0 \sum \tau_i L_{Ci} \quad (11)$$

$$R_{C3} = R_5 + R_6 + R_7 \quad (12)$$

expressed by equation (12).

$A_{G2}$ : Effective design sectional area of the grout in the non-steel section of the pile

$f_B$ : Yield strength of the core reinforcing bar

$\tau_i$ : Frictional strength at the perimeter surface of layer (i) that is considered to be affected by the frictional forces at the perimeter surface of the anchor part of the steel pipe section of the pile

$L_{Ci}$ : Thickness of the layer that is affected by the frictional forces at the perimeter surface of the anchor part of the steel pipe section of the pile

In most cases, Critical Condition 1 will determine the ultimate push-in bearing capacity. However, according to equation (1), the allowable push-in bearing

capacity  $R_{ca}$  is computed with the single safety factor  $n$ , although the ultimate push-in bearing capacity  $R_{cu}$  changes with  $R_{c1}$ ,  $R_{c2}$ , and  $R_{c3}$ .

In this way, the Current Design Guidelines (proposed) do not distinguish between the fluctuation levels of uncertain elements in the strength of the pile body itself, the frictional forces at the perimeter surface against the ground, and the operating load. The Guidelines simply use a single safety factor. We believe that by giving differentiated safety factors corresponding to each category of fluctuation level, significant improvements can be made to enhance safety levels.

In view of the above considerations, this paper attempts to apply the Partial Factor Design Method, which gives differentiated safety factors to each characteristic value of load and strength.

## (2) Partial Factor Design Method

Performance functions  $Z$  and  $Z_i$  corresponding to the entire system and to

$$Z = \min[R_{C1}, R_{C2}, R_{C3}] - S_D - S_E \quad (13)$$

$$Z_1 = R_1 + R_2 - S_D - S_E \quad (14)$$

$$Z_2 = R_3 + R_4 - S_D - S_E \quad (15)$$

$$Z_3 = R_5 + R_6 + R_7 - S_D - S_E \quad (16)$$

each of the Critical Conditions are defined in the following equations (13), (14), (15), and (16):

$$Z, Z_i > 0 \quad \text{Safe}$$

$$Z, Z_i \leq 0 \quad \text{Failure}$$

$S_D$  : Dead Load     $S_E$  : Earthquake Load  
Equations (17), (18) and (19) can be used as the design standard equations by

$$\phi_{R1}R_1^* + \phi_{R2}R_2^* \geq \gamma_{SD1}S_D^* + \gamma_{SE1}S_E^* \quad (17)$$

$$\phi_{R3}R_3^* + \phi_{R4}R_4^* \geq \gamma_{SD2}S_D^* + \gamma_{SE2}S_E^* \quad (18)$$

$$\phi_{R5}R_5^* + \phi_{R6}R_6^* + \phi_{R7}R_7^* \geq \gamma_{SD3}S_D^* + \gamma_{SE3}S_E^* \quad (19)$$

using partial factors for the performance function  $Z_i$ .

$R_j^*$  : Characteristic Value of each resisting force

$$(j=1,2,3,4,5,6, \text{ and } 7)$$

$S_D$  : Characteristic value of the dead load

$S_E$  : Characteristic value of the earthquake load

In order to make equations (14), (15) and (16) and equations (17),(18), and (19) equivalent to each other, partial factors  $\phi_{Rj}$ ,  $\gamma_{SDi}$ ,  $\gamma_{SEi}$  are derived with reference to Reliability Design Practice<sup>10</sup>,

$$\phi_{Rj} = \frac{1 - \alpha_{Rj}^T \beta_i^T V_{Rj}}{1 - k_{Rj} V_{Rj}} \quad (20)$$

$$\gamma_{SDi} = \frac{1 + \alpha_{SDi}^T \beta_i^T V_{SD}}{1 + k_{SDi} V_{SD}} \quad (21)$$

$$\gamma_{SEi} = \frac{1 + \alpha_{SEi}^T \beta_i^T V_{SE}}{1 + k_{SEi} V_{SE}} \quad (22)$$

as shown below. Details of partial factor introduction are given in Appendix.

$\alpha_{Rj}^T$  : Design sensitivity coefficient for each resisting force

$\beta_i^T$  : Target safety index for  $Z_i$

$K_{Rj}$  : Average coefficient for each resisting

force and characteristic values

$V_{Rj}$  : Fluctuation coefficient for each resisting force

$\alpha_{SDi}^T$  : Design sensitivity coefficient for the dead load

$V_{SD}$  : Fluctuation coefficient for the dead load

$k_{SDi}$  : Average dead load coefficient and characteristic values

$\alpha_{SEi}^T$  : Design sensitivity coefficient for the earthquake load

$V_{SE}$  : Fluctuation coefficient for the earthquake load

$k_{SEi}$  : Average earthquake load coefficient and characteristic values

Design sensitivity coefficients  $\alpha_{Rj}^T$ ,  $\alpha_{SDi}^T$ ,  $\alpha_{SEi}^T$  are determined in order to save computational time and costs, and the coefficients are derived from the distributions of  $\alpha_{Rj}$ ,  $\alpha_{SDi}$ , and  $\alpha_{SEi}$ <sup>16)</sup>.

$\alpha_{Rj}$ ,  $\alpha_{SDi}$ , and  $\alpha_{SEi}$  are given by equations (23), (24), and (25). The coefficients show the ratio of the individual standard deviations of the probability variables that contribute to

$$\alpha_{Rj} = \frac{\sigma_{Rj}}{\sigma_{Zi}} \quad (23)$$

the value of the standard deviation of the performance function  $Z_i$ .

Here, referring to equations (14), (15) and (16), when (i) = 1, j = 1, 2. Similarly, when

$$\alpha_{SDi} = \frac{\sigma_{SDi}}{\sigma_{Zi}} \quad (24)$$

$$\beta_i = \frac{\mu_{Zi}}{\sigma_{Zi}} \quad (26)$$

(i) = 2, j = 3, 4; and when (i) = 3, j = 5, 6, 7.

The target safety index  $\beta_i^T$  is to ensure safety by specifying the target value of  $\beta_i$  and is given by the following formula.

Here,  $\mu_{Zi}$  is the expected value of  $Z_i$  or the average of  $Z_i$ .

In Partial Factor Design, appropriate consideration must be given to determining the target safety index, the design sensitivity coefficient, and the fluctuation coefficient.

### 3. Characteristics of the Push-in Bearing Capacity

In order to clarify the probabilistic nature of the push-in bearing capacity, this section examines how the bearing capacity is influenced by changes in factors such as ground type and pile length.

The following variables are chosen as probability variables, with a large magnitude of uncertainty:  $\tau_i$ , q,  $f_G$ ,  $f_B$ ,  $f_C$ ,  $S_D$ ,  $S_E$ . Table 2 shows the chosen probability variables. The fluctuation coefficient  $\tau_i$  does not depend on the layer, and is given as 0.45 in reference to the relationships of the fluctuations in the N-value.<sup>15)</sup> Therefore  $R_i$  in equation

Table 2 Nature of Probability

Probability variable	Average/Characteristic values	Fluctuation coefficient $\nu$	Distribution shape	References
$\tau_i$	1.0	0.45	normal distribution	17
q	1.0	0.45	normal distribution	
$f_G$	1.0	0.30	normal distribution	18, 19
$f_B$	1.0	0.03	normal distribution	
$f_C$	1.0	0.03	normal distribution	20
$S_D$	1.0	0.10	normal distribution	
$S_E$	1.0	0.66	normal distribution	21



(3) is a linear equation in  $\tau_i$ .  $\tau_i$  is normally determined based on data obtained through sounding experiments, and for this reason the fluctuation coefficient  $R_1$  is set at 0.45 as in the case of the N-value.

$R_2$  is also a linear equation in  $q$ , and  $q$  is set at 0.45 for the same reason. Similarly, the fluctuation coefficients  $f_G, f_B, f_C, S_D, S_E$  are determined referring to documents<sup>16),17)</sup> and the fluctuation coefficients  $R_3 \sim R_6$  are derived. Based on the documents, all the probability variables are assumed to be normally distributed, although a rigorous analysis has not been carried out.

According to the Current Design Guidelines (proposed), the correction coefficient  $a$  is set at 1.00, 1.25, and 1.50, depending on the method used to pour the grout. Here, an average value of 1.25 is chosen. The dead load  $S_D$  and the earthquake load  $S/E$  operating on the pile are set at 400 (kN), the average value of each load, considering that the allowable bearing capacity in the event of an earthquake is some 1000 (kN), and that the average operating load should be significantly less than this.<sup>9)</sup>

First, Critical Condition 1 is examined based on the specific conditions assumed in actual cases. In Critical Condition 1, the anchor length  $L$  and the ground type are considered to be the most influential factors in determining the push-in bearing capacity. The three main types of

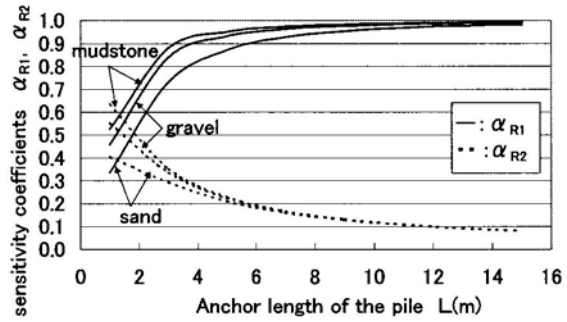


Figure 7  
Effect of anchor length on sensitivity coefficients in different types of ground

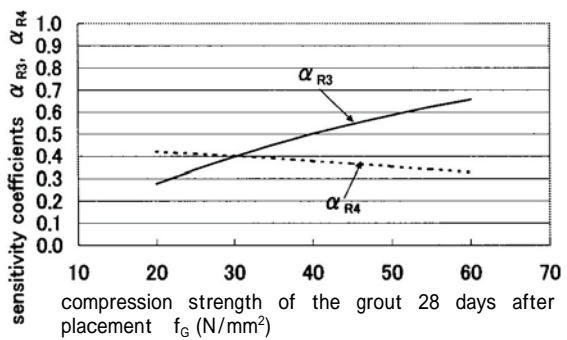


Figure 8  
Effect of compression strength of the grout on sensitivity coefficients 28 days after placement

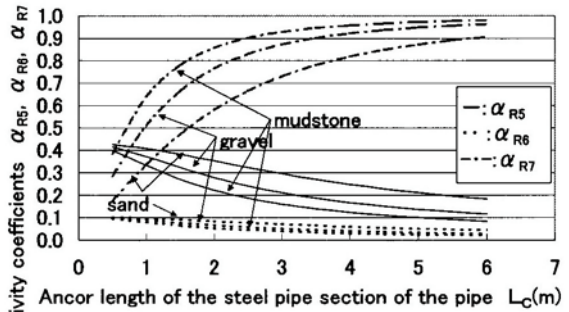


Figure 9  
Effect of anchor length of the steel pipe section of the pile,  $L_c$  on the sensitivity coefficients for different types of ground

material used for HMP; sand ( $\tau_i = 3\text{N/mm}^2$ ), gravel ( $\tau_i = 5\text{N/mm}^2$ ), and mudstone ( $\tau_i = 7\text{N/mm}^2$ ) are chosen and the changes in the sensitivity coefficients  $\alpha_{R1}$ , and  $\alpha_{R2}$  are studied with ground that has a uniform N-value of 50 for varied anchor lengths,  $L$ . Figure 7 shows the relationship between  $L$  on the

horizontal axis and  $\alpha_{R1}$  and  $\alpha_{R2}$  on the vertical axis.

Figure 7 shows that regardless of the ground type or anchor length,  $\alpha_{R1}$  is always dominant. Namely in Critical Condition 1,  $R_1$  is considered to be an influential factor in determining the push-in bearing capacity.

Next, Critical Condition 2 is analyzed. The Current Design Guidelines (proposed) stipulate that steel pipes and irregularly-shaped reinforcing bars used for HMPs should meet the shape specifications shown in Table 1. Regarding the characteristics for Critical Condition 2, the compression strength of the grout 28 days after placement  $f_G$  is chosen as the major factor, and its relationship with the sensitivity coefficients  $\alpha_{R3}$  and  $\alpha_{R4}$  is studied. The results are shown in Figure 8.

According to the Current Design Guidelines (proposed), in order to fully utilize the performance of the core reinforcing bar, it is recommended that cement milk or mortar of 30 (N/mm<sup>2</sup>) or more be used to obtain the required value for  $f_G$ .

In the domain where  $f_G$  reaches 30 (N/mm<sup>2</sup>) or more,  $\alpha_{R3}$  becomes dominant, and  $R_3$  is considered to be an influential factor in the push-in bearing capacity under Critical Condition 2.

Our analysis of Critical Condition 3 was also carried out for three types of ground as for Critical Condition 1. Equation (12)

shows that only  $R_7$  is affected by the ground conditions. The relationships between the anchor length of the steel pipe  $L_C$  and the sensitivity coefficients  $\alpha_{R5}$ ,  $\alpha_{R6}$ ,  $\alpha_{R7}$  are shown in Figure 9.

Figure 9 indicates that regardless of the ground type,  $\alpha_{R7}$  increases with  $L_C$ . The Current Design Guidelines (proposed) stipulate that the minimum required length of  $L_C$  is 1 meter in order for the axial force of the pipe to be transmitted to the grout in a stable way.<sup>9)</sup> Where  $L_C$  is 1 meter or more,  $\alpha_{R7}$  is always the largest sensitivity coefficient except for sandy ground. Even in sandy ground, from near the point 1.2 meters or more,  $\alpha_{R7}$  becomes the largest sensitivity coefficient. Therefore under Critical Condition 3,  $\alpha_{R7}$  is the most influential factor in determining the push-in bearing capacity.

#### 4. Determining the Target Safety Index and Design Sensitivity Coefficients

The target safety index  $\beta_a^T$ ,  $\beta_i^T$  and the design sensitivity coefficients  $\alpha_{Rj}^T$ ,  $\alpha_{SDi}^T$ , and  $\alpha_{SEi}^T$  are determined as follows: first the ground conditions are specified referring to the documents <sup>12),17),18),19)</sup> and 43 HMP samples are designed in Table 3 according to the Current Design Guidelines (proposed). The anchor ground is classified into the three categories: sand, gravel, and mudstone. A reliability analysis is carried out on these

Table 3 Pile lengths and ground conditions for the 43 HMP

sample NO.	Dimensions (m) of the pile		Thickness of the anchor ground Li (m)		Frictional strength (N/mm <sup>2</sup> )		Strength of material and correction coefficient		External force (kN)	
	L	Lc	L <sub>1</sub>	L <sub>2</sub>	1	2	a	f <sub>G</sub> (N/mm <sup>2</sup> )	S <sub>D</sub>	S <sub>E</sub>
1	9.0	1.2	4.9	4.1	3.5	4.4	1.50	32.0	343.6	351.3
2	8.0	1.3	4.4	3.6	3.9	5.1	1.50	35.5	310.7	430.4
3	10.0	1.1	8.0	-	5.9	-	1.50	32.1	411.9	361.6
4	9.0	1.2	7.5	1.5	3.9	4.9	1.50	36.0	468.8	382.0
5	7.4	1.0	7.4	-	4.4	-	1.00	38.1	483.7	415.9
6	7.7	1.5	7.7	-	5.5	-	1.25	40.0	331.2	397.9
7	7.5	1.7	3.5	4.0	4.4	5.4	1.25	32.0	394.9	422.3
8	7.1	1.1	4.0	3.1	3.9	6.4	1.00	31.4	372.0	393.1
9	7.0	1.4	4.0	3.0	4.4	6.9	1.25	38.1	345.5	440.5
10	7.1	1.2	5.0	2.1	4.4	6.4	1.00	31.8	439.7	437.7
11	7.6	2.0	7.6	-	4.4	-	1.00	37.1	311.6	384.8
12	7.6	1.9	3.6	4.0	3.9	5.9	1.00	32.4	403.8	407.0
13	7.1	1.7	5.9	1.2	3.7	5.9	1.00	31.2	408.1	437.2
14	9.0	1.6	6.2	2.8	3.5	4.9	1.50	31.5	452.7	427.1
15	8.5	1.3	4.5	4.0	4.4	5.6	1.25	41.4	410.0	371.8
16	9.0	1.6	6.4	2.6	3.9	4.4	1.25	36.6	394.3	383.6
17	7.9	1.3	5.6	2.3	4.4	4.9	1.25	35.6	465.8	393.5
18	8.0	1.3	5.0	3.0	3.7	4.9	1.00	32.5	489.0	420.4
19	7.1	1.1	7.1	-	3.9	-	1.25	37.3	436.3	396.3
20	6.9	1.6	1.4	5.5	4.2	5.8	1.00	32.9	483.5	352.2
21	7.6	1.2	4.0	3.6	4.0	5.9	1.00	32.1	352.2	385.4
22	7.0	1.9	4.7	3.2	4.9	5.7	1.00	34.7	377.5	425.8
23	8.1	1.0	8.1	-	4.1	-	1.25	39.0	470.3	418.7
24	7.6	1.7	4.6	3.0	4.7	5.3	1.50	39.9	422.0	361.8
25	7.0	1.5	3.4	3.6	4.9	5.9	1.00	31.8	470.7	419.5
26	7.4	1.2	2.7	4.7	3.9	4.9	1.00	41.4	482.5	360.8
27	8.6	1.6	8.6	-	3.9	-	1.25	39.5	326.3	399.8
28	7.1	1.6	1.2	5.9	4.0	4.4	1.25	31.8	462.2	373.8
29	7.4	1.7	7.4	-	5.5	-	1.25	33.5	471.7	383.4
30	7.3	1.7	2.8	4.5	4.4	5.3	1.25	40.2	351.6	440.2
31	7.3	1.5	7.3	-	2.9	-	1.50	40.2	365.3	401.6
32	10.6	3.7	7.7	2.9	1.3	3.4	1.50	30.0	310.7	411.9
33	11.1	3.9	10.0	1.1	1.4	6.8	1.50	38.9	483.7	331.2
34	12.9	3.1	5.0	7.9	2.5	2.5	1.50	35.1	372.0	345.5
35	9.9	1.5	6.0	3.9	1.8	2.6	1.50	37.4	311.6	403.8
36	10.2	1.9	1.9	8.3	3.1	3.1	1.50	35.8	452.7	410.0
37	11.6	3.3	6.0	5.6	2.0	2.6	1.50	37.3	483.5	352.2
38	11.1	4.7	15.0	-	2.6	-	1.50	34.3	470.3	422.0
39	18.0	5.0	5.0	13.0	2.1	2.1	1.50	39.0	482.5	326.3
40	7.5	1.2	2.0	5.5	2.2	3.4	1.50	39.4	375.3	354.5
41	6.9	1.6	4.0	2.9	1.2	6.7	1.50	35.1	371.5	448.8
42	9.1	2.8	7.5	1.6	2.1	6.1	1.50	36.9	400.7	410.1
43	4.8	1.5	1.1	3.7	6.5	6.5	1.50	30.9	413.5	378.7

43 samples and their distributions are studied.

In this section, the probability variables are  $\tau_i$ ,  $q$ ,  $f_G$ ,  $f_B$ ,  $f_C$ ,  $S_D$ ,  $S_E$  and the same values are assumed for the fluctuation coefficients, the same as in the preceding section. With the above considerations, the distribution of the safety index is examined and valid target safety index values are determined.

(1) Determining the target safety index

$$\beta_a^T, \text{ and } \beta_i^T$$

In order to determine the target safety index  $\beta_a^T$  for the entire system, the distribution of the safety index  $\beta_a$  for the 43 HMP samples is examined. First, the failure probability  $P_f$  for the entire system is derived by the Monte Carlo simulation method<sup>10)</sup> for the 43 HMP samples. The Monte Carlo simulation method is a numerical experiment that

repeats an experiment a number of times using random numbers to determine the

$\phi(\beta)$  is the probability function for a normal distribution with a mean of zero

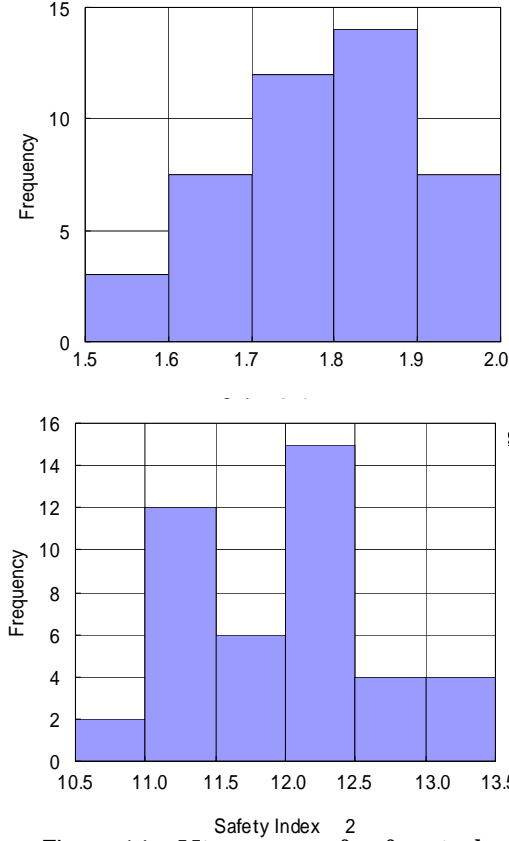


Figure 14 Histogram of safety index  $\beta_2$  for Critical Condition 2

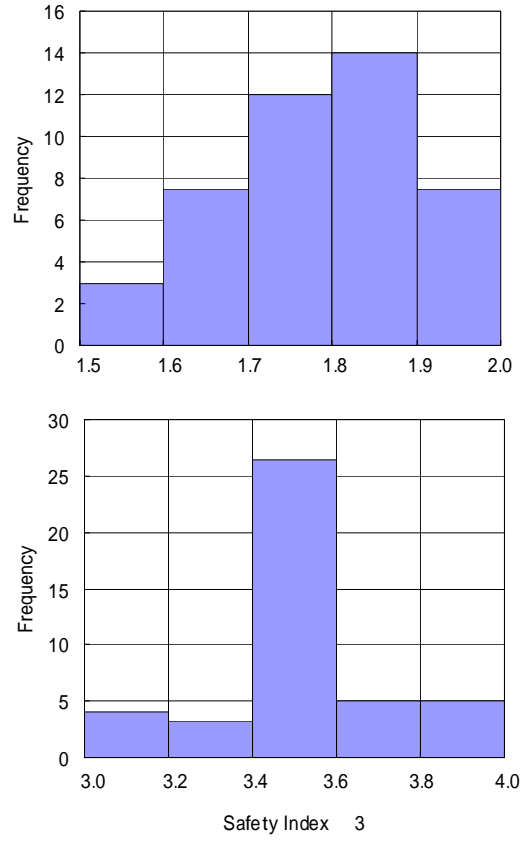


Figure 13 Histogram of safety index  $\beta_3$  for Critical Condition 3

probability of a failure. The Monte Carlo simulation method defines the failure probability  $P_f$  as the number of failures divided by the number of trials, providing that the number of trials is at least 300000.

The number of failures depends on the three Critical Conditions, 1, 2, and 3.  $\beta$  and  $\beta_a$  are derived from equation (27) showing the relation between  $P_f$ , and a histogram of  $\beta_a$  is drawn as shown in Figure 10.

$$P_f = 1 - \Phi(\beta) \quad (27)$$

and a standard deviation of 1.0. In the histogram in Figure 10, the mean of  $\beta_a$ , i.e.  $\mu_{\beta_a}$ , and the standard deviation  $\sigma_{\beta_a}$  are computed as 1.79 and 0.12 respectively. This paper sets up the target safety index in a more strict way and  $\beta_a^T$  is set to 1.85, the sum of  $\mu_{\beta_a}$  and  $\sigma_{\beta_a}/2$  in order that the safety criteria in the Current Design Guidelines (proposed) are compatible with the present paper, although the number 1.85 may need further justification.

Next, the safety index  $\beta_i$  is computed from equation (26) for the 43 HMP

samples and the histograms in Figures 11, 12, and 13 show the distribution for each condition. Comparing Figure 11 to Figure 10,  $\beta_a$  for the entire system is determined by Critical Condition 1. However, there is a difference between  $\beta_a$  and  $\beta_1$  due to the difference in the method used for the Monte Carlo simulation, to the theoretical equations used, and to the effects of Critical Condition 3 onto  $\beta_a$ .

A closer look at the distribution of  $\beta_2$ , show that it is extremely large compared to  $\beta_1$  and  $\beta_3$ . Thus sufficient safety is ensured. Critical Condition 2 presents no dominant factors affecting the push-in bearing capacity, and a detailed examination was not made. From here on, the critical condition is neglected. Though  $\beta_3$  is larger than  $\beta_1$ , this paper employs 5.0 as the safety index, in line with European standards for the allowable safety index. Our detailed examination is made up to this level. From here on, Critical Condition 3 is examined.

The target safety indexes  $\beta_1$ ,  $\beta_3$ ,  $\beta_1^T$ ,  $\beta_3^T$  are determined in the same way as for  $\beta_a^T$ . Table 4 shows the target safety indexes  $\beta^T$ ,  $\beta_1^T$ , and  $\beta_3^T$  thus determined.

Table 4 Target safety index

$\beta_a^T$	1.85
$\beta_1^T$	1.85
$\beta_3^T$	3.62

(2) Determining the design sensitivity

coefficients  $\alpha_j^T$ ,  $\alpha_{SD}^T$ ,  $\alpha_{SE}^T$

The sensitivity coefficients  $\alpha_{R1}$ ,  $\alpha_{R2}$ ,  $\alpha_{SD1}$ ,  $\alpha_{SE1}$  for Critical Condition 1 for the 43 HMP samples are computed using equations (23), (24), and (25). The ultimate bearing capacity  $R_{c1}^*$  and its relationship to the sensitivity coefficients is examined, with the results shown in Figure 14. The figure shows the trend lines. Taking a closer look at the lines, the gradients of all the lines are moderate, and the sensitivity coefficients make small changes with changes in the magnitude of  $R_{c1}^*$ . Therefore, this paper determines the design sensitivity coefficients  $\alpha_{R1}^T$ ,  $\alpha_{R2}^T$ ,  $\alpha_{SD1}^T$ ,  $\alpha_{SE1}^T$  as the average of the values of  $\alpha_{R1}$ ,  $\alpha_{R2}$ ,  $\alpha_{SD1}$ ,  $\alpha_{SE1}$ , which are computed from the

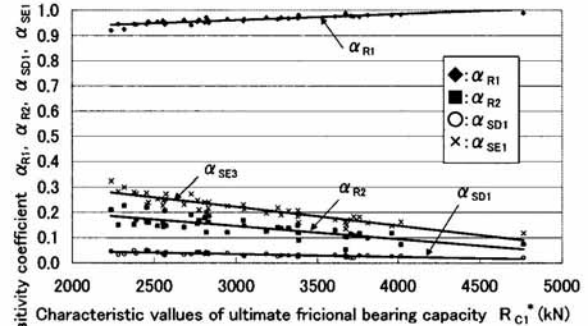


Figure 14 Relationship between sensitivity

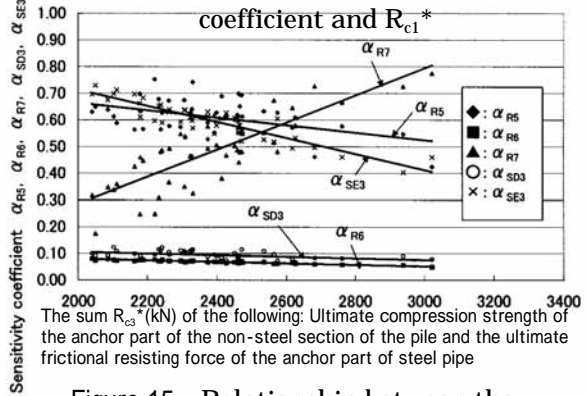


Figure 15 Relationship between the sensitivity coefficient and  $R_{c3}^*$

43 HMP samples. It is noted that the

value of  $\alpha_{SE1}^T$  is arranged so that the total sum of the following should exceed 1.0 by some amount: ( $\alpha_{R1}^T$ ) raised to the power of 2, ( $\alpha_{R2}^T$ ) raised to the power of 2, ( $\alpha_{SD1}^T$ ) raised to the power of 2, and ( $\alpha_{SE1}^T$ ) raised to the power of 2.

This is because that the safety index is over-evaluated when the sum of the sensitivity coefficients, each raised to the power of 2, exceeds 1.0.

For Critical Condition 3, we examined the relationship between the sensitivity coefficients  $\alpha_{R5}$ ,  $\alpha_{R6}$ ,  $\alpha_{R7}$ ,  $\alpha_{SD3}$ ,  $\alpha_{SE3}$  and the sum of the ultimate compression strength of the anchor part of the non-steel section of the pile and the ultimate frictional resisting forces of the anchor part of the steel pipe section of the pile. The results are shown in Figure 15. Looking at the trends for  $\alpha_{R7}$  and  $\alpha_{SE3}$ , the gradient is significantly steep. Namely, the sensitivity coefficients  $\alpha_{R7}$  and  $\alpha_{SE3}$  are influenced by the magnitude of  $R_{C3}^*$ . Therefore the design sensitivity coefficients  $\alpha_{R7}^T$  and  $\alpha_{SE3}^T$  are fixed by classifying the magnitude of  $R_{C3}^*$  into several categories because of this influence. It is noted that  $\alpha_{R5}^T$ ,  $\alpha_{R6}^T$ ,  $\alpha_{SD3}^T$  are set as the average of the sensitivity coefficients computed from the 43 HMP samples, due to the small gradient of the sensitivity lines.  $\alpha_{SD3}^T$  is determined as in the case of  $\alpha_{SE1}^T$ .

Table 5 shows the design sensitivity

coefficients thus determined.

## 5 Designing an HMP by the Partial Factor Design Method

### (1) Designing an HMP by the Partial Factor Design Method

In this section, partial factors  $\phi_{Rj}$ ,  $\gamma_{SDi}$ ,  $\gamma_{SEi}$  are computed and the 43 HMP samples are designed using the Partial Factor Design Method. They are then compared with the results shown in the last section, where the same samples were designed using the Current Design Guidelines (proposed).

Table 6 shows the results for the partial factors,  $\phi_{Rj}$ ,  $\gamma_{SDi}$ ,  $\gamma_{SEi}$  computed from equations (20), (21) and (22), using the values for the fluctuation coefficients  $V_{Rj}$ ,  $V_{SD}$  and  $V_{SE}$  fixed in section 3, and values for the target safety index  $\beta_i^T$  and design

Table 5 Design sensitivity coefficient

$R_1^T$	$R_2^T$	$SD_1^T$	$SE_1^T$
0.963	0.142	0.034	0.24

$R_{C3}^*$ (kN)	$R_5^T$	$R_6^T$	$R_7^T$	$SD_3^T$	$SE_3^T$
~ 2600	0.610	0.069	0.267	0.094	0.74
2600 ~			0.567		0.545

Table 6 Partial Factors

$R_1$	$R_2$	$SD_1$	$SE_1$
0.198	0.882	1.006	1.293

$R_{C3}^*$ (kN)	$R_5$	$R_6$	$R_7$	$SE_1$	$SE_1$
~ 2600	0.338	0.992	0.566	1.034	2.768
2600 ~			0.076		2.302

sensitivity coefficients  $\alpha_j^T$ ,  $\alpha_{SDi}^T$ ,  $\alpha_{SEi}^T$  determined in the last section. It is noted

that an average is taken of the individual values.

Comparing the safety factor under the Current Design Guidelines with the partial factors here, the safety factor on the side of the bearing capacity is uniformly 0.5 in the Guidelines, imposing severe restrictions on design, while the partial factor  $\phi_{R1}$  of the main bearing capacity  $R_1^*$  in Critical Condition 1 is 0.198, giving much more freedom. Also in Critical Condition 3, a similar difference is found in the domain where  $R_{C3}^*$  is 2600kN or more, although there is no difference between the safety factor and  $\phi_{R7}$  when  $R_{C3}^*$  is 2600kN or less.

Next the same 43 sample HMPs are designed using the partial factors  $\phi_{Rj}$ ,  $\gamma_{SDi}$ ,  $\gamma_{SEi}$  and the design standard equations (17) and (19). In Critical Condition 1, the design variable is assumed to be the anchor length L, and in Critical Condition 3, the design variable is assumed to be the anchor length of the steel pipe.

In designing the anchor length L, an inequality is formed for L by substituting the characteristic values of each element, i.e. the average values, into the design standard equation (17). Then, giving an initial value of 0.1 meters to L and extending the length of the bearing ground in 0.1 meter increments, the minimum length of L that satisfies the inequality can be computed, and the minimum length thus obtained is fixed as

the anchor length L' designed by the Partial Factor Design Method.

Similarly,  $L_c$  is designed by substituting the characteristic values of each element except  $L_c$  into the design standard equation (19) and by forming an inequality. The initial value of  $L_c$  is set as 0.1 meters and is incremented by 0.1 meters, and the minimum value of  $L_c$  that satisfies the inequality is computed and is taken as the anchor length of the steel pipe designed by the Partial Factor Design Method. However, note that in order to be compatible with the Current Design Guidelines (proposed), the minimum length  $L_c'$  is set at 1.0 meters to follow the requirement in the Guidelines that the axial force of the steel pipe must be transmitted to the grout in a reliable way.

The safety indexes  $\beta_i'$ ,  $\beta_a'$  are computed in order to examine the degree of safety of the HMP designed by the Partial Factor Design Method, as in section 4.

(2) Study on the safety of HMPs designed by the Partial Factor Design Method

A comparison is made with regard to the safety of the HMP between the Current Design Guidelines (proposed) and the Partial Factor Design Method. This is done by showing the distribution of  $\beta_i'$ , and  $\beta_a'$  for each Critical Condition. Note, however that  $\beta$  has some deviations because  $\beta$  is varied with each individual HMP designed according

to the Current Design Guidelines (proposed). On the other hand  $\beta'$  has less deviation because  $\beta'$  is computed by applying partial factors to each element of load/intensity for  $\beta^T$ . Figure 16 compares  $\beta_1$  and  $\beta_1'$  and Figure 17 compares  $\beta_3$  and  $\beta_3'$ .

According to Figure 16,  $\beta_1'$  is more concentrated at the target safety index of Critical Condition 1,  $\beta_1^T$  than  $\beta_1$  is.

Meanwhile, Figure 17 shows that no difference was found in the safety index between  $\beta_3$  and  $\beta_3'$ , although  $\beta_3'$  shows large deviations. The wide deviations are thought to be due to the fact that Critical Condition 3 does not impose a critical impact and the dimensions of the HMP cannot be determined.

For the HMP designed by the Partial Factor Design Method, Figure 18 shows a comparison between  $\beta_a'$ , which is the safety index of the entire system derived in the same method as in section 4, and  $\beta_a$ . Figure 18 shows that  $\beta_a'$  has fewer deviations than  $\beta_a$  and  $\beta_a'$  is more concentrated at  $\beta_a^T$ . It follows that the HMP designed by the Partial Factor Design Method ensures sufficient safety for the push-in bearing capacity.

## 6. Summary and Conclusions

Having studied the uncertainty in the component elements of the push-in bearing capacity for three critical

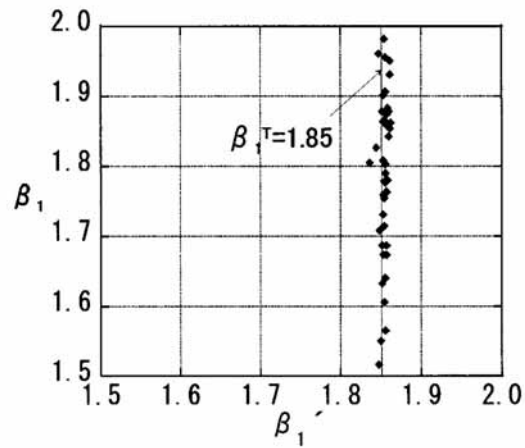


Figure 16 Comparison of  $\beta_1$  and  $\beta_1'$

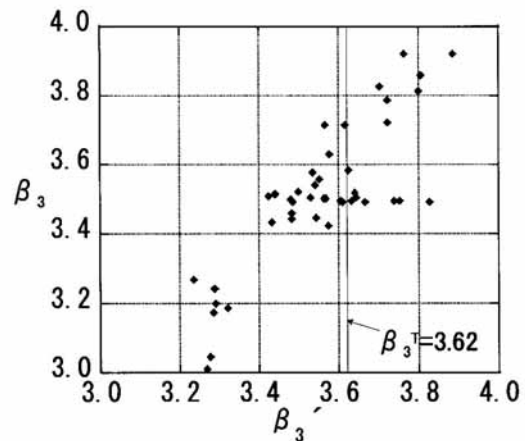


Figure 17 Comparison of  $\beta_3$  and  $\beta_3'$

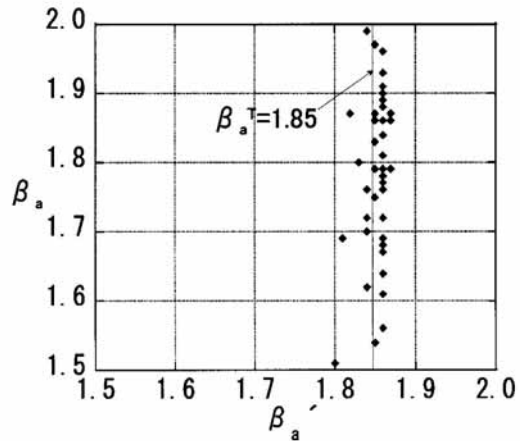


Figure 18 Comparison of  $\beta_a$  and  $\beta_a'$

conditions based on probability theory, and having also examined the use of the Partial Factor Design Method in HMP design, we have reached the following conclusions:

- (1) The safety indexes  $\beta_a$  and  $\beta_i$  for the



push-in bearing capacity of an HMP designed by the Current Design Guidelines and the sensitivity coefficients  $\alpha_{Rj}$ ,  $\alpha_{SDi}$ ,  $\alpha_{SEi}$  were computed and their distributions were clarified. It was established that a detailed examination is not required for critical condition 2, because the condition does not have a critical impact.

(2) The target safety indexes  $\beta^T$  and  $\beta_i^T$  and the design sensitivity coefficients  $\alpha_{Rj}^T$ ,  $\alpha_{SDi}^T$ ,  $\alpha_{SEi}^T$  were determined using the results in (1) above. The HMP samples were designed by the Partial Factor Design Method. The safety indexes  $\beta_a'$ ,  $\beta_r'$  were computed and their distributions were compared. It was confirmed that except for  $\beta_3'$ ,  $\beta_a'$  and  $\beta_i'$  are concentrated at  $\beta_a^T$  and  $\beta_i^T$  respectively. It was also clarified from a comparison of the distributions of  $\beta_3$  and  $\beta_3'$  that a detailed examination is not required for critical condition 3, because the condition does not have a critical impact.

(3) It was clarified that a detailed examination is not required for critical conditions 2 and 3 in determining the push-in bearing capacity of the HMP, and that a detailed examination for critical condition 1 alone is sufficient. Namely as shown in Figure 16, the distribution of  $\beta_i'$  is concentrated at  $\beta_i^T$  and a dependable level of safety can secured

with due consideration to the uncertainty of each e  $\beta_i \geq \beta_i^T$  (A·4)

Factor Design method.

(4) For the c the sections Design is c analysis flo should be

$$\frac{1 - \alpha_{R1} \beta_1^T V_{R1}}{1 - k_{R1} V_{R1}} R_1^* + \frac{1 - \alpha_{R2} \beta_1^T V_{R2}}{1 - k_{R2} V_{R2}} R_2^* \geq \frac{1 + \alpha_{SD1} \beta_1^T V_{SD}}{1 + k_{SD1} V_{SD}} S_D^* + \frac{1 + \alpha_{SE1} \beta_1^T V_{SE}}{1 + k_{SE1} V_{SE}} S_E^* \quad (A \cdot 12)$$

application is chosen for the 43 HMP samples, their loads, and the characteristics of the ground. It follows that the application of the Partial Factor Design Method should be limited to within a certain framework. Therefore it is not recommended that the Partial Factor Design Method employed in this paper be applied to HMP design using data which is out of scope.

## Appendix

Here we show how partial factors are derived for Critical Condition 1.

The partial factors  $\phi_{R1}$ ,  $\phi_{R2}$ ,  $\gamma_{S1}$ ,  $\gamma_{S2}$  need to be determined so that design standard equation (17) for Critical Condition 1 is compatible with the performance function of Critical Condition 1; i.e., equation (14).

In the design,

The above equation needs to be satisfied

$$\mu_{Z1} = \mu_{R1} + \mu_{R2} - \mu_{SD} - \mu_{SE} \quad (A \cdot 1)$$

$$\sigma_{Z1}^2 = \sigma_{R1}^2 + \sigma_{R2}^2 + \sigma_{SD}^2 + \sigma_{SE}^2 \quad (A \cdot 2)$$

$$\beta_1 = \frac{\mu_{R1} + \mu_{R2} - \mu_{SD} - \mu_{SE}}{\sqrt{\sigma_{R1}^2 + \sigma_{R2}^2 + \sigma_{SD}^2 + \sigma_{SE}^2}} = \frac{\mu_{Z1}}{\sigma_{Z1}} \quad (A \cdot 3)$$

and equation (A-3) is substituted into equation (A-4) to give the following equation (A-5).

Here,

Equation (A-5) can be expressed in the form of equation (A-7) by using the above

$$\mu_{R1} + \mu_{R2} - \mu_{SD} - \mu_{SE} \geq \beta_1^T \sqrt{\sigma_{R1}^2 + \sigma_{R2}^2 + \sigma_{SD}^2 + \sigma_{SE}^2} \quad (A \cdot 5)$$

approximation for equation (A-6).

$$\sqrt{\sigma_{R1}^2 + \sigma_{R2}^2 + \sigma_{SD1}^2 + \sigma_{SE1}^2} \equiv \alpha_{R1}\sigma_{R1} + \alpha_{R2}\sigma_{R2} + \alpha_{SD1}\sigma_{SD} + \alpha_{SE1}\sigma_{SE} \quad (A \cdot 6)$$

Substituting the fluctuation coefficients in equation (A-7) gives

Here the characteristic values are used as

$$\mu_{R1} + \mu_{R2} - \mu_{SD1} - \mu_{SE1} \geq \beta_1^T \left( \begin{array}{c} \alpha_{R1}\sigma_{R1} + \alpha_{R2}\sigma_{R2} \\ + \alpha_{SD1}\sigma_{SD} + \alpha_{SE1}\sigma_{SE} \end{array} \right) \quad (A \cdot 7)$$

the nominal values. For example,  $R_1^*$  and  $S_{D1}^*$  can be expressed as in equation (A-

$$\mu_{R1} + \mu_{R2} - \mu_{SD} - \mu_{SE} \geq \beta_1^T \left( \begin{array}{c} \alpha_{R1} V_{R1} \mu_{R1} + \alpha_{R2} V_{R2} \mu_{R2} \\ + \alpha_{SD1} V_{SD} \mu_{SD} + \alpha_{SE1} V_{SE} \mu_{SE} \end{array} \right) \quad (A \cdot 8)$$

$$\begin{aligned} & (1 - \alpha_{R1} \beta_1^T V_{R1}) \mu_{R1} + (1 - \alpha_{R2} \beta_1^T V_{R2}) \mu_{R2} \\ & \geq (1 + \alpha_{SD1} \beta_1^T V_{SD}) \mu_{SD} + (1 + \alpha_{SE1} \beta_1^T V_{SE}) \mu_{SE} \end{aligned} \quad (A \cdot 9)$$

10) and equation (A-11) respectively.

Equation (A-9) can be reduced to (A-12) by using the characteristic values in (A-9).

$$R_1^* = (1 - k_{R1} V_{R1}) \mu_{R1} \quad (A \cdot 10)$$

$$S_{SD}^* = (1 + k_{SD1} V_{SD}) \mu_{SD} \quad (A \cdot 11)$$

The partial factors are expressed by equations (A-13), (A-14), (A-15), and (A-16) from equation (17) and equation (A-12).

If the HMP designer/user has to use the values each time from the above equations to compute the sensitivity coefficients, this can become a problem, particularly for users who have insufficient knowledge of the fundamentals of probability theory.

Therefore, to simplify the process in this

$$\phi_{R1} = \frac{1 - \alpha_{R1} \beta_1^T V_{R1}}{1 - k_{R1} V_{R1}} \quad (A \cdot 13)$$

$$\phi_{R2} = \frac{1 - \alpha_{R2} \beta_1^T V_{R2}}{1 - k_{R2} V_{R2}} \quad (A \cdot 14)$$

$$\gamma_{SD1} = \frac{1 + \alpha_{SD1} \beta_1^T V_{SD}}{1 + k_{SD1} V_{SD}} \quad (A \cdot 15)$$

$$\gamma_{SE1} = \frac{1 + \alpha_{SE1} \beta_1^T V_{SE}}{1 + k_{SE1} V_{SE}} \quad (A \cdot 16)$$

paper, the sensitivity coefficients are unified in order to unify the partial factors into one, so that they can easily be computed. Thus, the partial factors are expressed by equations (A-17), (A-18), (A-19) and (A-20).

## References

- 1) Federal Highway Administration, U.S. Department of Transportation: Drilled and Grouted Micropiles: State of Practice Review, Volume I : Background, Classifications, Cost, Pub.No.FHWA-RD-96-016, July, 1997.

$$\phi_{R1} = \frac{1 - \alpha_{R1}^T \beta_1^T V_{R1}}{1 - k_{R1} V_{R1}} \quad (\text{A}\cdot 17)$$

$$\phi_{R2} = \frac{1 - \alpha_{R2}^T \beta_1^T V_{R2}}{1 - k_{R2} V_{R2}} \quad (\text{A}\cdot 18)$$

$$\gamma_{SD1} = \frac{1 + \alpha_{SD1}^T \beta_1^T V_{SD}}{1 + k_{SD1} V_{SD}} \quad (\text{A}\cdot 19)$$

$$\gamma_{SE1} = \frac{1 + \alpha_{SE1}^T \beta_1^T V_{SE}}{1 + k_{SE1} V_{SE}} \quad (\text{A}\cdot 20)$$

- 2) Federal Highway Administration, U.S.Department of Transportation: Drilled and Grouted Micropiles: State of Practice Review, Volume IV: Case Histories, Pub.No.FHWA-RD-96-019,July,1997.
- 3) Henning Muhra: Micropiles in Northern and Middle Europe, Pub. No. 39, Geotechnical Laboratory, Tampere University of Technology, 1997.
- 4) F.Lizzi: The static restoration of monuments, Sadep Publisher, pp.70,1982.
- 5) Proc. of First International Workshop on Micropiles, Doubletree Inn, Seattle, Washington, September, 1997.
- 6) Proc. of 3<sup>rd</sup> IWM2000, Geotechnical Laboratory, Tampere University of Technology, Finland, June, 2000.
- 7) Takahiro Kishishita, Ethuro Saito, Yoshinori Otani, Fusanori Miura, Masaki Yato: Seismic Retrofitting of Existing Structural Foundation by High-Capacity Micro Piles, The 10<sup>th</sup> Japan Earthquake Engineering Symposium, Vol.1,pp161-166,1998.11.
- 8) Yoshinori Otani , Makoto Mega, Seiji Hamathuka: Case histories of Micropiles, The Foundation Engineering & Equipment, Vol.26,No.7,1998
- 9) Japan Association of high-capacity Micro Piles: Design and Construction Manual of High-capacity Micro Piles (draft), 1999
- 10) Masaru Hoshiya, Kiyoshi Ishii : Reliability based design of structure, Kajima Institute Publishing Co., Ltd. ,1986
- 11) Eurocode 1-Basis of design and actions on structure part 1:Basis of design, 1994.
- 12) Makoto Suzuki: Exercise for bearing capacity of piles, Technical committee of structure engineering; Japan society of civil engineers, 1999
- 13) Japan Road Association: Reference for highway bridge design specifications for highway bridges Part IV; Substructures, 1999
- 14) ISO2394; General principles on reliability for structures, Reference No. ISO/FDIS 2394,1988.
- 15) Kenji Mathui: Bearing capacity of friction piles with consideration of uncertainty of soil properties, CTI Engineering Co., Ltd.,1992
- 16) Architectural Institute of Japan: , Report about Ultimate Strength Design Method for reinforced concrete, 1987
- 17) Japan Road Association: Report about the earthquake-proof design of a highway bridge, 1997
- 18) Jiro Fukui, Masahiro Nishitani, Takeshi Umebara and Takeo Miki: Study on the Retrofitting of Bridge

Foundations with Micropile, Second International Workshop on Micropiles Proceeding, pp73-pp82, '99IWM Executive Committee, Yamaguchi University, October,1999.

- 19) Federal Highway Administration, U.S.Department of Transportation: Drilled and Grouted Micropiles: State of Practice Review, Volume II: Design, Pub.No.FHWA-RD-96-017, July,1997.